THE JOURNAL OF PHYSICAL CHEMISTRY B

Article

pubs.acs.org/JPCB

Role of Ionic Liquid on the Conformational Dynamics in the Native, Molten Globule, and Unfolded States of Cytochrome C: A Fluorescence Correlation Spectroscopy Study

Supratik Sen Mojumdar, Rajdeep Chowdhury, Shyamtanu Chattoraj, and Kankan Bhattacharyya*

Department of Physical Chemistry, Indian Association for the Cultivation of Science, Jadavpur, Kolkata-700032, India

ABSTRACT: The role of a room temperature ionic liquid (RTIL, [pmim][Br]) on the size and conformational dynamics of a protein, horse heart cytochrome c (Cyt C) in its native, molten globule (MG-I and II), and unfolded states is studied using fluorescence correlation spectroscopy (FCS). For this purpose, the protein was covalently labeled by a fluorescent dye, Alexa Fluor 488. It is observed that the addition of the RTIL leads to an increase in the hydrodynamic radius (r_H) of the protein, Cyt C in the native or MG-I state. In contrast, the addition of RTIL causes a decrease in the size (hydrodynamic radius, r_H) of Cyt C unfolded by GdnHCl or MG-II state. The decrease in size indicates the formation of a relatively compact structure. We detected two types of conformational relaxation of the protein. The shorter relaxation time component (~3−5.5 μs) corresponds to the protein folding or intrachain contact formation, while the relatively longer time component (~63−122 μs) may be assigned to the motion of the protein side chains or concerted chain dynamics. The burst integrated fluorescence lifetime histograms indicate that the increase in size of the protein is accompanied by an increase in the contribution of the shorter component (~0.3−0.4 ns) with a concomitant decrease of the contribution of the longer component (~2.8−3.6 ns). An opposite trend is observed during the decrease in size of the protein.

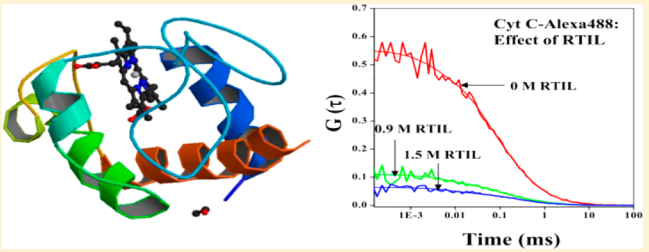

1. INTRODUCTION

In recent years, fluorescence correlation spectroscopy (FCS) has been extensively applied to study conformational fluctuations in RNA,[1,2] DNA,[3−7] polypeptides,[8] and proteins.[9−15] The structure of a protein is not rigid and fluctuates constantly. As a result of this fluctuation, the distances between different residues vary with time. This causes fluctuation in the efficiency of FRET between two probes attached covalently to different residues.[16−18] Conformational fluctuations also affect electron transfer in a protein.[19−21] The amino group of a residue (e.g., tryptophan, tyrosin etc.) quenches fluorescence of a covalent probe by electron transfer when it comes in close contact during conformational fluctuation of the protein. This leads to fluctuation of fluorescence intensity. The time scale of fluctuation may be obtained from the FCS data. Using this principle, Webb and co-workers detected three components of the conformational relaxation of apomyoglobin and compared the relaxation components in folded and unfolded states of the protein.[9] Chattopadhyay et al. studied the conformational dynamics of a fatty acid binding protein and detected a single conformational relaxation time.[10,11] Lu and co-workers observed inhomogeneous conformational fluctuation in an intracellular signaling protein complex and studied its implication in enzyme kinetics.[16,22] Dynamical fluctuations of both conformation and enzyme activity in a single protein occur in a wide time scale (~100 μs to 10 s).[23]

Most recently, we have investigated the role of RTIL on the native and denatured state of human serum albumin (HSA) covalently labeled at the cysteine-34 by a malemide dye (CPM).[15] We observed that both 1.5 M RTIL and 6 M GdnHCl separately cause an increase in hydrodynamic radius (r_H) from ~38 Å in the absence of RTIL (or GdnHCl) to ~61 Å in the presence of 1.5 M RTIL or 6 M GdnHCl. When RTIL is added to the HSA denatured by 6 M GdnHCl, the hydrodynamic radius (r_H) decreases from ~61 Å to ~41 Å indicating formation of a relatively compact structure (folded state).[15] Thus, the RTIL helps the unfolded protein to refold and displays a protein stabilizing behavior (like an osmolyte).[24,25] Of course, size alone does not indicate the biological function.

In the present work, we focus on a respiratory protein, horse heart Cytochrome C (Cyt C). Horse heart Cyt C is a small heme protein (104 residues, ~12 KDa) which may be covalently labeled by a fluorophore (e.g., Alexa Fluor 488). In principle, the probe Alexa may bind to a solvent exposed amino acid that contains a free primary amino group (e.g., lysine). However, many groups have shown that Cyt C contains a lysine-rich region around the heme crevice, and Alexa can bind to this site of the protein.[26,27] Cyt C has a single tryptophan residue (Trp-59) which efficiently quenches fluorescence of the fluorophore along with other weak quenchers such as Tyr, Met, and His during conformational fluctuation.[28,29] Horse heart Cyt

Received: July 24, 2012
Revised: September 11, 2012
Published: September 18, 2012

C forms two well-known molten globule or folding intermediate states (MG-I and MG-II) where the protein stays for a long time.[12] MG-I is formed in the presence of 2 mM SDS, while MG-II is formed on addition of 2 mM SDS and 5 M urea.[26,30]

Because of its involvement in important apoptosis,[30] non-native states of Cyt C have received special attention. Chattopadhyay and co-workers studied the effect of protein stabilizers (e.g., arginine and sodium perchlorate) on the conformational dynamics of the unfolded state of yeast Cyt C and its early folding kinetics using FCS and MEM methods.[24,25] They showed that the addition of arginine causes a decrease in hydrodynamic radius (r_H) of yeast Cyt C both in the native and unfolded state. They fit the FCS data to a single relaxation component and reported a ~30 μs component which varies with urea concentrations. Majima and co-workers reported two kinds of motion, one (~1.5 μs) due to segmental motion and other (~55 μs) due to folding dynamics of the unfolded Cyt C.[29] Large scale molecular dynamics simulation reports different time scales of concerted motion and chain dynamics of Cyt C.[31,32]

Though many groups have studied conformational dynamics of Cyt C both in native and denatured state, there is hardly any report on the effect of RTIL on the native, denatured, and partially unfolded states of Cyt C. In the present study, we investigate the role of RTIL on the conformational dynamics of horse heart Cyt C in its native, denatured, and molten globule (partially unfolded) states using a single molecule technique (FCS).

2. EXPERIMENTAL METHODS

2.1. Protein Labeling and Sample Preparation for the FCS Experiment. We labeled horse heart Cyt C (Scheme 1A) by Alexa Fluor 488 carboxylic acid TFP ester (purchased from Sigma Aldrich and Invitrogen, respectively, and used without any further purification, Scheme 1B). Labeling was carried out by the procedure as described in Alexa Fluor 488 Protein Labeling Kit, obtained from Molecular Probes (Invitrogen), and also the protocol described by Kam and Dai.[33] Briefly, 1 M solution of sodium bicarbonate buffer of pH ~ 9.0 was prepared. The protein was diluted to 2 mg/mL in 0.1 M sodium bicarbonate buffer and mixed with the provided dye. Then, the reaction mixture was stirred for 1 h at room temperature.

Scheme 1. Structure of (A) Horse Heart Cyt C (Data from Protein Data Bank; pdb ID: 1hrc), (B) Alexa Fluor 488 Carboxylic Acid, TFP Ester, and (C) [pmim][Br]

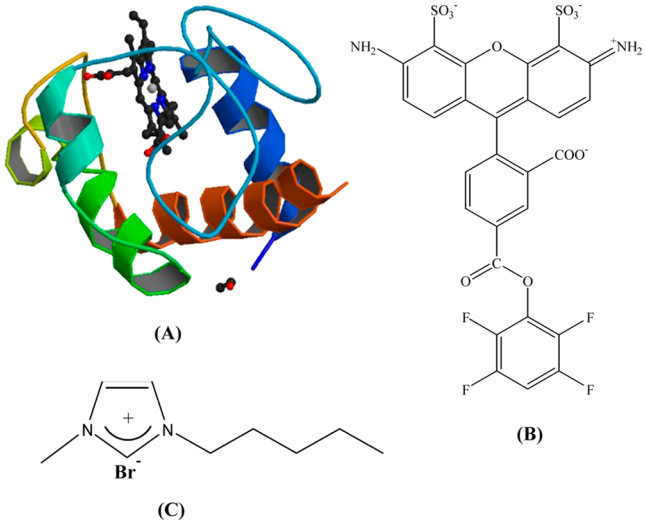

PBS elution buffer was prepared at room temperature. The buffer contained 0.1 M potassium phosphate and 1.5 M NaCl with 2 mM sodium azide (pH ~ 7.2). The homogeneous purification resin (Bio-Rad BioGel P-30 fine size exclusion purification resin, designed to separate free dye from proteins) was pipetted into the column, allowing excess buffer to drain away.

The solution was filtered through the column by continuous addition of the elution buffer until the labeled protein had been eluted. We illuminated the column with a hand-held UV lamp periodically and observed two colored bands, which represent the separation of labeled protein from unincorporated dye. We collected the first colored band, which contains the labeled protein.

For the FCS experiment, we diluted the solution such that the probe concentration was kept at about ~1 nM. In the FCS experiment, Tween-20 (0.05%) was used as a solvent additive to suppress attachment of the protein to the glass surface. The pH of the solution was kept at 7.0; all of the FCS experiments were carried out at 20 °C, and laser power was kept at ~65 μW.

2.2. FCS Measurements. FCS studies of the protein samples (~1 nM Alexa 488) were carried out in a confocal setup (PicoQuant, MicroTime 200) with an inverted optical microscope-Olympus IX-71. A water immersion objective (60 × 1.2 NA) was used to focus the excitation light (470 nm) from a pulsed diode laser (PDL 828-S "SEPIA II," PicoQuant) onto the sample placed on a coverslip (~50 μL). The fluorophore was excited at 470 nm using a picosecond diode with stable repetition rate (40 MHz). To separate the fluorescence from the exciting laser (along the same path) we used a dichroic mirror (490dcxr, chroma) and appropriate band-pass filters (HQ500lp, Chroma). The fluorescence was then focused through a pinhole (50 μm) onto a 50/50 beam splitter prior to entering two single photon avalanche diodes (SPADs). The fluorescence autocorrelation traces were recorded by using two detectors. The signal was subsequently processed by the PicoHarp-300 time-correlated single photon counting card (PicoQuant) to generate the autocorrelation function, $G(\tau)$. The data were collected in time-tagged time-resolved (TTTR) mode.

2.3. FCS Data Modeling and Analysis. In FCS, the autocorrelation function $G(\tau)$ of fluorescence intensity is defined as:

$$G(\tau) = \frac{\langle \delta F(0)\delta F(\tau)\rangle}{\langle F\rangle^2} \quad (1)$$

where $\langle F\rangle$ is the average intensity and $\delta F(\tau)$ is the fluctuation in intensity at a delay τ around the mean value; that is, $\delta F(\tau) = \langle F\rangle - F(\tau)$. In case of free diffusion of a two-state fluorophore diffusing in a 3D Gaussian excitation volume of widths ω_{xy} and ω_z,

$$G_D(\tau) = \frac{1}{N}\left[1 + \frac{\tau}{\tau_D}\right]^{-1}\left[1 + \frac{\tau}{\omega^2\tau_D}\right]^{-1/2} \quad (2)$$

where N is the number of molecules in the observed volume, τ_D is the diffusion time of the species

Table 1. Size and Conformational Time Components of Native (Cyt C-Alexa 488) and Molten Globule States of Cyt C

system	A_1	$\tau_{R_1}{}^a$ (μs)		A_2	$\tau_{R_2}{}^a$ (μs)		τ_D (μs)	r_H (Å)
		$\tau_{R_1}^{uncorr}$	$\tau_{R_1}^{corr}$		$\tau_{R_2}^{uncorr}$	$\tau_{R_2}^{corr}$		
native Cyt C	25%	3.0	3.0	75%	63.0	63.0	295 ± 20	18.6 ± 1.0
Cyt C + 2 mM SDS (MG-I)	40%	3.2	2.9	60%	75.0	67.0	400 ± 45	22.4 ± 2.5
Cyt C + 2 mM SDS + 5 M urea (MG-II)	40%	7.0	4.8	60%	160.0	110.0	607 ± 30	26.4 ± 1.5

[a] ±10%.

Table 2. Effect of RTIL on the Native State (Cyt C-Alexa 488)

system	A_1	$\tau_{R_1}{}^a$ (μs)		A_2	$\tau_{R_2}{}^a$ (μs)		τ_D (μs)	r_H (Å)
		$\tau_{R_1}^{uncorr}$	$\tau_{R_1}^{corr}$		$\tau_{R_2}^{uncorr}$	$\tau_{R_2}^{corr}$		
native Cyt C	25%	3.0	3.0	75%	63.0	63.0	295 ± 20	18.6 ± 1.0
Cyt C + 0.3 M RTIL	40%	5.5	5.1	60%	90.0	84.0	343 ± 25	20.1 ± 1.5
Cyt C + 0.9 M RTIL	45%	9.6	5.4	55%	174	97.0	657 ± 35	23.2 ± 1.0
Cyt C + 1.5 M RTIL	35%	11.0	5.0	65%	256	114	900 ± 55	25.2 ± 2.0

[a] ±10%.

$$\tau_D = \frac{\omega_{xy}^2}{4D_t} \tag{3}$$

and $\omega = \omega_z/\omega_{xy}$ which is the height-to-diameter ratio of the 3D Gaussian confocal volume. The structure parameter (ω) of the excitation volume was calibrated using a sample (R6G in water) of known diffusion coefficient (D_t = 426 μm^2 s^{-1}).[34] The estimated volume of the excitation volume is ~1.36 fL with a transverse radius (ω_{xy}) ~ 365 nm. If the sample is undergoing conformational fluctuation among the multiple states, then they can be distinguished by their fluorescence quantum yield. We assume that there is no detectable change in τ_D among the states, then the correlation function

$$G(t) = G_D(\tau)G_F(\tau) \tag{4}$$

where $G_F(\tau)$ is the contribution from conformational fluctuation to the correlation function. For two-component conformational relaxation, $G_F(\tau)$ can be defined as,

$$G_F(\tau) = [1 + A_1 e^{-\tau/\tau_{R_1}} + A_2 e^{-\tau/\tau_{R_2}}] \tag{5}$$

where τ_R is the relaxation time for an exponential component with an associated amplitude A. Combining the contributions to the correlation function caused by diffusion ($G_D(\tau)$) and those caused by the conformational fluctuations of the protein ($G_F(\tau)$), the actual autocorrelation function ($G(\tau)$) can be defined as,[9]

$$G(\tau) = \frac{1}{N}\left[1 + \frac{\tau}{\tau_D}\right]^{-1}\left[1 + \frac{\tau}{\omega^2\tau_D}\right]^{-1/2} \times [1 + A_1 e^{-\tau/\tau_{R_1}} + A_2 e^{-\tau/\tau_{R_2}}] \tag{6}$$

We analyzed all of the raw FCS data by a fitting software IgorPro 6. The correlation function data for all the systems can be fit successfully by using the eq 5. We call it a single diffusion and two-component conformational relaxation model.

According to the Stokes–Einstein equation, r_H can be determined from the measured value of D_t of the diffusing species as follows,

$$D_t = \frac{k_B T}{6\pi\eta r_H} \tag{7}$$

where η is the viscosity of the solution and r_H is the hydrodynamic radius.

The addition of RTIL (Scheme 1C), GdnHCl, SDS, or urea significantly changes the viscosity and refractive index of the medium, and hence, affects the accurate determination of size of the proteins (r_H). We have corrected the refractive index mismatch and viscosity effect to accurately measure the hydrodynamic radius (r_H) of the protein. The correction was done following the discussions by Chattopadhyay et al.[35] and Sherman et al.[36] Sherman et al.[36] used R6G as a diffusion standard and used ratio method to eliminate the errors due to refractive index mismatch and viscosity. We also chose R6G as a diffusion standard and used the following equation,[36]

$$\frac{r_H^{protein}}{r_H^{R6G}} = \frac{\tau_D^{protein}}{\tau_D^{R6G}} \tag{8}$$

Since R6G is a rigid molecule, its r_H is independent of refractive index and viscosity. r_H of R6G was determined using eq 7 from the known value of D_t of R6G in bulk water (426 $\mu m^2/s$).[34] We determined the diffusion time of free R6G in different solutions of GdnHCl, RTIL, SDS, and urea at different concentrations without the protein sample for each experiment. The standardization with free R6G probe mimics the exact experimental condition to minimize the effect due to viscosity and the refractive index. We have also corrected the relaxation time constants (τ_i) for viscosity (η) of the medium using the formula,

$$\tau_i^{corr} = \tau_i^{uncorr} \times \frac{\eta_{buffer}}{\eta_{sample}} = \tau_i^{uncorr} \times \frac{\tau_D^{buffer}}{\tau_D^{sample}} \tag{9}$$

where, τ_i^{corr} is the viscosity corrected relaxation time components, τ_i^{uncorr} denotes the viscosity uncorrected relaxation time components, and τ_D^{buffer} and τ_D^{sample} are diffusion times of R6G in buffer and different sample solutions, respectively.

3. RESULTS

3.1. Size of Horse Heart Cyt C: FCS Study. In this section, we discuss how the size of the protein varies in the native, unfolded, and molten globule states on addition of RTIL. We fit the FCS data with two components of conformational relaxation along with a diffusive component

dx.doi.org/10.1021/jp307297s | J. Phys. Chem. B 2012, 116, 12189–12198

Table 3. Effect of GdnHCl on the Native State (Cyt C-Alexa 488)

system	A_1	$\tau_{R_1}{}^a$ (μs)		A_2	$\tau_{R_2}{}^a$ (μs)		τ_D (μs)	r_H (Å)
		$\tau_{R_1}^{uncorr}$	$\tau_{R_1}^{corr}$		$\tau_{R_2}^{uncorr}$	$\tau_{R_2}^{corr}$		
native Cyt C	25%	3.0	3.0	75%	63.0	63.0	295 ± 20	18.6 ± 1.0
Cyt C + 1.5 M GdnHCl	25%	3.8	3.5	75%	85.0	78.0	420 ± 45	24.4 ± 2.5
Cyt C + 2.5 M GdnHCl	40%	5.0	4.4	60%	118	105	480 ± 40	26.9 ± 2.0
Cyt C + 4 M GdnHCl	20%	5.5	4.4	80%	144	115	570 ± 30	29 ± 1.5
Cyt C + 6 M GdnHCl	25%	6.5	4.4	75%	180	122	709 ± 65	30.3 ± 2.5

[a] ±10%.

Table 4. Effect of RTIL on the Denatured State (Cyt C-Alexa 488 + 6 M GdnHCl)

system	A_1	$\tau_{R_1}{}^a$ (μs)		A_2	$\tau_{R_2}{}^a$ (μs)		τ_D (μs)	r_H (Å)
		$\tau_{R_1}^{uncorr}$	$\tau_{R_1}^{corr}$		$\tau_{R_2}^{uncorr}$	$\tau_{R_2}^{corr}$		
native Cyt C	25%	3.0	3.0	75%	63.0	63.0	295 ± 20	18.6 ± 1.0
Cyt C + 6 M GdnHCl	25%	6.5	4.4	75%	180.0	122.0	709 ± 65	30.3 ± 2.5
Cyt C + 6 M GdnHCl + 0.3 M RTIL	45%	7.9	4.2	55%	219.0	118.0	849 ± 45	29.3 ± 1.5
Cyt C + 6 M GdnHCl + 0.9 M RTIL	35%	9.2	3.7	65%	268.0	107.0	1113 ± 75	27.6 ± 2.0
Cyt C + 6 M GdnHCl + 1.5 M RTIL	35%	10.0	3.4	65%	290.0	98.0	1202 ± 90	25.3 ± 2.0

[a] ±10%.

Table 5. Effect of RTIL on the Molten Globule State I (Cyt C-Alexa 488 + 2 mM SDS)

system	A_1	$\tau_{R_1}{}^a$ (μs)		A_2	$\tau_{R_2}{}^a$ (μs)		τ_D (μs)	r_H (Å)
		$\tau_{R_1}^{uncorr}$	$\tau_{R_1}^{corr}$		$\tau_{R_2}^{uncorr}$	$\tau_{R_2}^{corr}$		
native Cyt C	25%	3.0	3.0	75%	63.0	63.0	295 ± 20	18.6 ± 1.0
Cyt C + 2 mM SDS (MG-I)	40%	3.2	2.9	60%	75.0	67.0	400 ± 45	22.4 ± 2.5
MG-I + 0.3 M RTIL	50%	6.2	4.7	50%	120.0	92.0	490 ± 25	23.5 ± 1.0
MG-I + 0.9 M RTIL	50%	8.5	4.7	50%	190.0	105.0	720 ± 35	25.0 ± 1.5
MG-I + 1.5 M RTIL	40%	10.5	4.5	60%	270.0	117.0	975 ± 40	26.6 ± 1.0

[a] ±10%.

Table 6. Effect of the RTIL on the Molten Globule State II (Cyt C-Alexa 488 + 2 mM SDS + 5 M Urea)

system	A_1	$\tau_{R_1}{}^a$ (μs)		A_2	$\tau_{R_2}{}^a$ (μs)		τ_D (μs)	r_H (Å)
		$\tau_{R_1}^{uncorr}$	$\tau_{R_1}^{corr}$		$\tau_{R_2}^{uncorr}$	$\tau_{R_2}^{corr}$		
native Cyt C	25%	3.0	3.0	75%	63.0	63.0	295 ± 20	18.6 ± 1.0
Cyt C + 2 mM SDS + 5 M urea (MG-II)	40%	7.0	4.8	60%	160.0	110.0	607 ± 30	26.4 ± 1.5
MG-II + 0.3 M RTIL	45%	8.0	4.4	55%	190.0	102.0	720 ± 45	24.4 ± 1.5
MG-II + 0.9 M RTIL	35%	10.5	4.0	65%	250.0	96.0	960 ± 70	22.9 ± 2.0
MG-II + 1.5 M RTIL	30%	11.0	3.5	70%	265.0	85.0	1050 ± 50	21.2 ± 1.0

[a] ±10%.

which gives the size (hydrodynamic radius) of the protein. Before discussing the results, it may be noted that with the gradual addition of additives (RTIL, GdnHCl, urea, or SDS) the number of molecules within the focal volume (N) increases. This is because of the increase of the confocal volume as a result of change in refractive index of the medium. The addition of different additives also causes an increase in the viscosity of the medium significantly. Thus, the measured τ_D overestimates the r_H. We corrected for both the factors (refractive index and viscosity) in this work as described in section 2.3 and calculated the r_H using eq 8. The diffusion times obtained from our measurement are summarized in Tables 1−6 along with the calculated r_H.

3.1.1. Size of Native and Molten Globule State of Horse Heart Cyt C. The hydrodynamic radius (r_H) of the protein can be calculated from the diffusion time (τ_D; obtained by fitting the FCS traces) using eq 8. For native Cyt C, we observed a diffusion time of 295 μs that corresponds to an r_H of 18.6 Å (Table 1). For the native (folded) state of a protein with N residues, Wilkins et al.[37] proposed an empirical formula, $r_H = 4.75N^{0.29}$ Å. According to this formula, the calculated r_H of horse heart Cyt C ($N \sim 104$) in the native (folded) state is ~17.8 Å. The observed r_H value (18.6 Å) for Cyt C is in good agreement with the theoretical value (17.8 Å).

We now discuss the size of the Cyt C in the two molten globule (partially unfolded) states (MG-I and MG-II). In first molten globule state, MG-I (formed in 2 mM SDS), from the FCS data the diffusion time is observed to be 400 μs, and r_H is measured to be 22.4 Å (Table 1). This indicates a ~20% increase in size compared to the native state of the protein.

For the second intermediate, the MG-II state (in 2 mM SDS and 5 M urea) of Cyt C, from the FCS data we obtained a diffusion time of 607 μs which corresponds to r_H of 26.4 Å (a ~42% increase in r_H compared to the native state; Table 1).

dx.doi.org/10.1021/jp307297s | J. Phys. Chem. B 2012, 116, 12189−12198

3.1.2. Effect of the RTIL on the Size of Cyt C. Figure 1 shows the FCS traces of native Cyt C in the presence of the

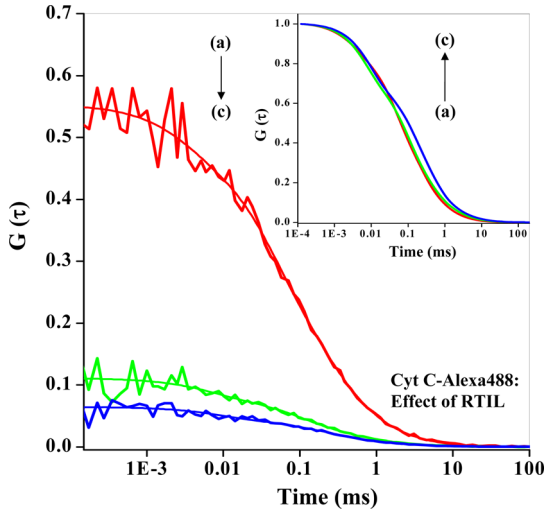

Figure 1. Autocorrelation traces with their best fit lines of Cyt C-Alexa 488 in (a) native condition (red) and after addition of (b) 0.9 M [pmim][Br] (green) and (c) 1.5 M [pmim][Br] (blue) to the native Cyt C. The inset shows the best fit lines.

RTIL. On addition of the RTIL to the protein, the diffusion time increases from ~295 μs (in native Cyt C) to ~900 μs (in presence of 1.5 M RTIL), and the hydrodynamic radius (r_H) increases from 18.6 Å (in native Cyt C) to 25.2 Å (in the presence of 1.5 M RTIL; Table 2).

According to Wilkins et al.[37] the r_H for a protein in the fully denatured state can be obtained using the relation, $r_H = 2.21N^{0.57}$. For horse heart Cyt C (N ~104), from this formula r_H is calculated to be 32.6 Å in the fully denatured state.[37] This is larger than the r_H (25.2 Å) observed in 1.5 M RTIL. Thus it appears that 1.5 M RTIL causes partial (~35% increase in r_H compared to that of the native state) but not complete unfolding of Cyt C.

3.1.3. Effect of GdnHCl on the Size of Cyt C. Figure 2 and Table 3 describe the effect of GdnHCl, a strong denaturant, on

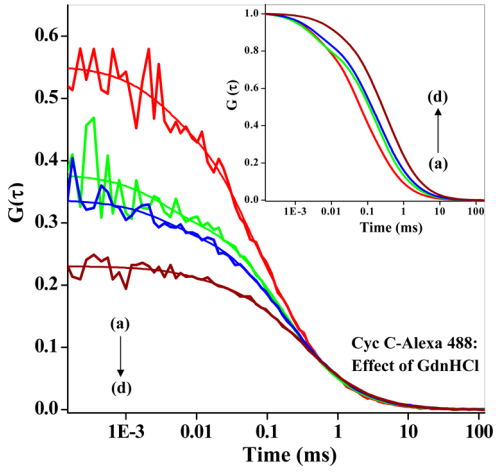

Figure 2. Autocorrelation traces with their best fit lines of Cyt C-Alexa 488 in (a) native condition (red) and after addition of (b) 1.5 M GdnHCl (green), (c) 2.5 M GdnHCl (blue), and (d) 6 M GdnHCl (wine) to the native Cyt C. The inset shows the best fit lines.

the diffusion time and hydrodynamic radius of Cyt C. In 6 M GdnHCl, the diffusion time (τ_D) of Cyt C is observed to be ~709 μs that corresponds to a r_H of 30.3 Å (~ 63% increase in r_H compared to that of native state). This is very close to the calculated r_H (32.6 Å)[37] of the fully denatured protein. Thus addition of 6 M GdnHCl causes almost complete unfolding of the protein. Thus, 6 M GdnHCl causes a greater amount of unfolding than the 1.5 M RTIL ([pmim][Br]). But, note at ~1.5 M GdnHCl the r_H of the protein (~ 24.4 Å) is almost similar to that of the protein (~25.2 Å) in 1.5 M RTIL. This observation is in good agreement that GdnHCl and halogen containing RTIL ([pmim][Br]) has a similar denaturing ability on a molar basis, as reported in earlier studies.[38,39]

3.1.4. Effect of the RTIL on the Size of Cyt C Denatured by 6 M GdnHCl. The hydrodynamic radius, r_H, of Cyt C increases from 18.6 Å in the native state to 30.3 Å in 6 M GdnHCl. On addition of the RTIL to the protein, denatured by 6 M GdnHCl, the hydrodynamic radius (r_H) decreases to ~29.3 Å in 0.3 M RTIL and to ~25.3 Å in 1.5 M RTIL (Figure 3, Table

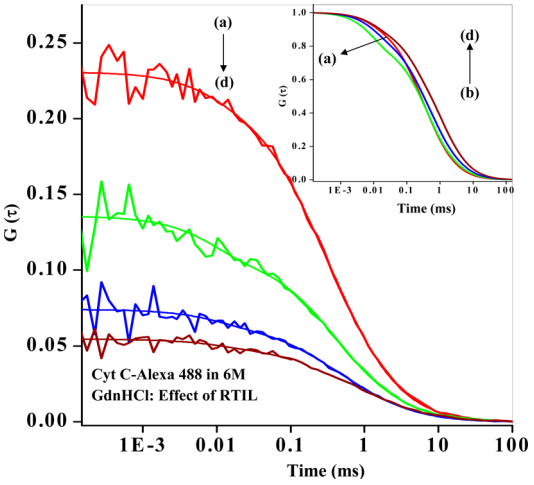

Figure 3. Autocorrelation traces with their best fit lines of Cyt C-Alexa 488 in (a) fully denatured condition (by 6 M GdnHCl) (red) and after addition of (b) 0.3 M [pmim][Br] (green), (c) 0.9 M [pmim][Br] (blue), and (d) 1.5 M [pmim][Br] (wine) to the denatured Cyt C. The inset shows the best fit lines.

4). Thus, addition of 1.5 M RTIL stabilizes the structure of the protein and recovers ~43% of the native structure (in size). However, in the case of Cyt C denatured by GdnHCl, 1.5 M RTIL does not completely recover the native structure of the protein (as it does in the case of HSA[15]). The folding intermediate of Cyt C(r_H ~ 25.3 Å) obtained in the presence of 1.5 M RTIL and 6 M GdnHCl resembles the intermediate (with r_H ~ 25.2 Å) obtained when 1.5 M RTIL is added to the protein.

3.1.5. Effect of the RTIL on the Size of Molten Globule States of Cyt C. The effect of the RTIL on the two molten globule states, MG-I and MG-II, is opposite to each other. In the case of MG-I, addition of the RTIL causes an increase in r_H from 22.4 Å in 0 M RTIL to 26.6 Å in 1.5 M RTIL. Thus the RTIL causes further unfolding of this partially folded structure (MG-I; Figure 4, Table 5).

When the RTIL is added to the second intermediate state, MG-II, the size (r_H) decreases from 26.4 Å in 0 M RTIL to 21.2 Å in 1.5 M RTIL. This indicates the formation of a relatively

dx.doi.org/10.1021/jp307297s | J. Phys. Chem. B 2012, 116, 12189−12198

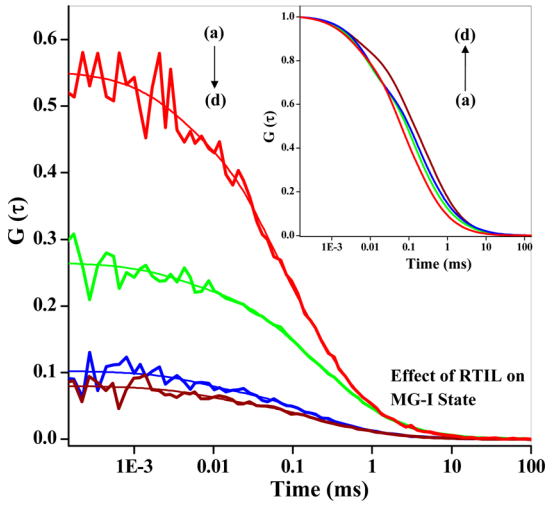

Figure 4. Autocorrelation traces with their best fit lines of Cyt C-Alexa 488 in (a) native condition (red) and (b) in presence of 2 mM SDS (MG-I state) (green) and after addition of (c) 0.9 M [pmim][Br] (blue) and (d) 1.5 M [pmim][Br] (wine) to the MG-I state. The inset shows the best fit lines.

compact structure of the intermediate MG-II in the presence of the RTIL (Figure 5, Table 6).

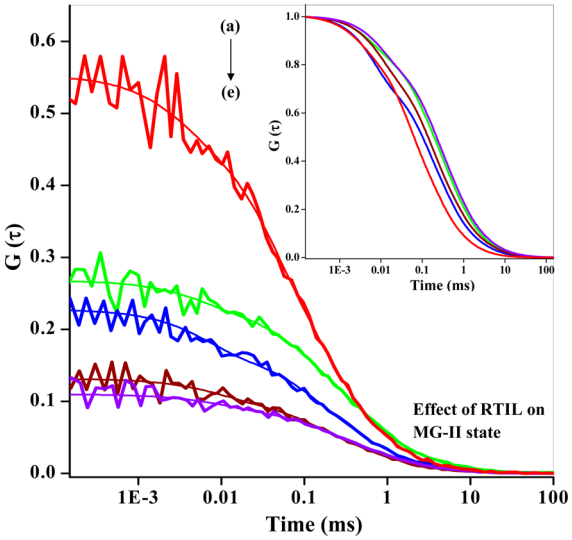

Figure 5. Autocorrelation traces with their best fit lines of Cyt C-Alexa 488 in (a) native condition (red) and (b) in the presence of 2 mM SDS + 5 M urea (MG-II state) (green) and after addition of (c) 0.3 M [pmim][Br] (blue), (d) 0.9 M [pmim][Br] (wine), and (e) 1.5 M [pmim][Br] (violet) to the MG-II state. The inset shows the best fit lines.

3.2. Conformational Dynamics. As mentioned earlier, we have fit the FCS curves to a model with single diffusion and two-component conformational relaxation. We obtained two relaxation times in each case. The results are summarized in Tables 1−6. It may be mentioned that the viscosity of the medium increases on addition of the RTIL and GdnHCl and other additives (SDS and urea). Therefore, in Tables 1−6 we have included both the uncorrected relaxation time along with viscosity corrected relaxation time calculated using eq 9.

3.2.1. Conformational Dynamics in the Native and Molten Globule States. In the native state of Cyt C, we found two components—3 and 63 μs (Table 1). The fastest component (3 μs) may be assigned to the segmental motion of the protein, while the relatively slower component (~63 μs) may be ascribed to the concerted chain motion or side chain dynamics of the protein polypeptide chain. We now compare time constants for conformational relaxation components in the two molten globule states to those in the native state of Cyt C.

For the molten globule state, MG-I, the viscosity uncorrected time constants are 3.2 and 75 μs (Table 1). The viscosity-corrected components of the conformational dynamics in the MG-I state are 2.9 and 67 μs (Table 1). These values of segmental motion (2.9 μs) and the side chain dynamics (~ 67 μs) of Cyt C polypeptide chains are very close to that of the native state (3 and 63 μs). This indicates that MG-I state contains residual structure with native-like compactness.

In the case of the MG-II state the viscosity corrected time components of the segmental motion (4.8 μs) and side chain dynamics (110 μs) are slower than those in the native state (Table 1). This shows that MG-II state is more unfolded and more labile and contains a smaller amount of native-like compactness.

3.2.2. Effect of the RTIL on Conformational Dynamics. The relaxation times of the protein increase on addition of RTIL. The viscosity-corrected relaxation times (~5 and 114 μs) in the presence of 1.5 M RTIL are slower than those (3 and 63 μs) in the native state of Cyt C (Table 2). As indicated in previous works,[10,11,40−42] the slower components involve diffusion of the protein side chains. Hence, in the unfolded protein, the side chains need to diffuse through a longer path to reach closer to the probe molecule to quench its fluorescence emission.

3.2.3. Effect of GdnHCl on Conformational Dynamics. The segmental motion as well as the concerted chain motion increases with the gradual addition of GdnHCl due to unfolding of the protein. The viscosity-corrected time constants in 6 M GdnHCl are 4.4 and 122 μs, which are ~1.5−2 fold slower compared to the corresponding relaxation times in the native state (Figure 6, Table 3).

3.2.4. Effect of the RTIL on the Conformational Dynamics in the Denatured State. When the RTIL is added to the Cyt C denatured by 6 M GdnHCl, conformational relaxation becomes significantly faster. On addition of 1.5 M RTIL to the denatured protein, the viscosity-corrected time constants are ~3.4 and

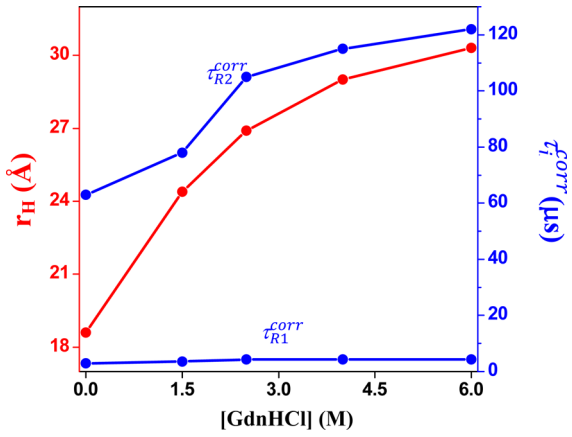

Figure 6. Plot of hydrodynamic radius (r_H, left *y*-axis, red)/viscosity-corrected relaxation time component (right *y*-axis, blue) vs concentration of GdnHCl added to the protein Cyt C.

dx.doi.org/10.1021/jp307297s | J. Phys. Chem. B 2012, 116, 12189−12198

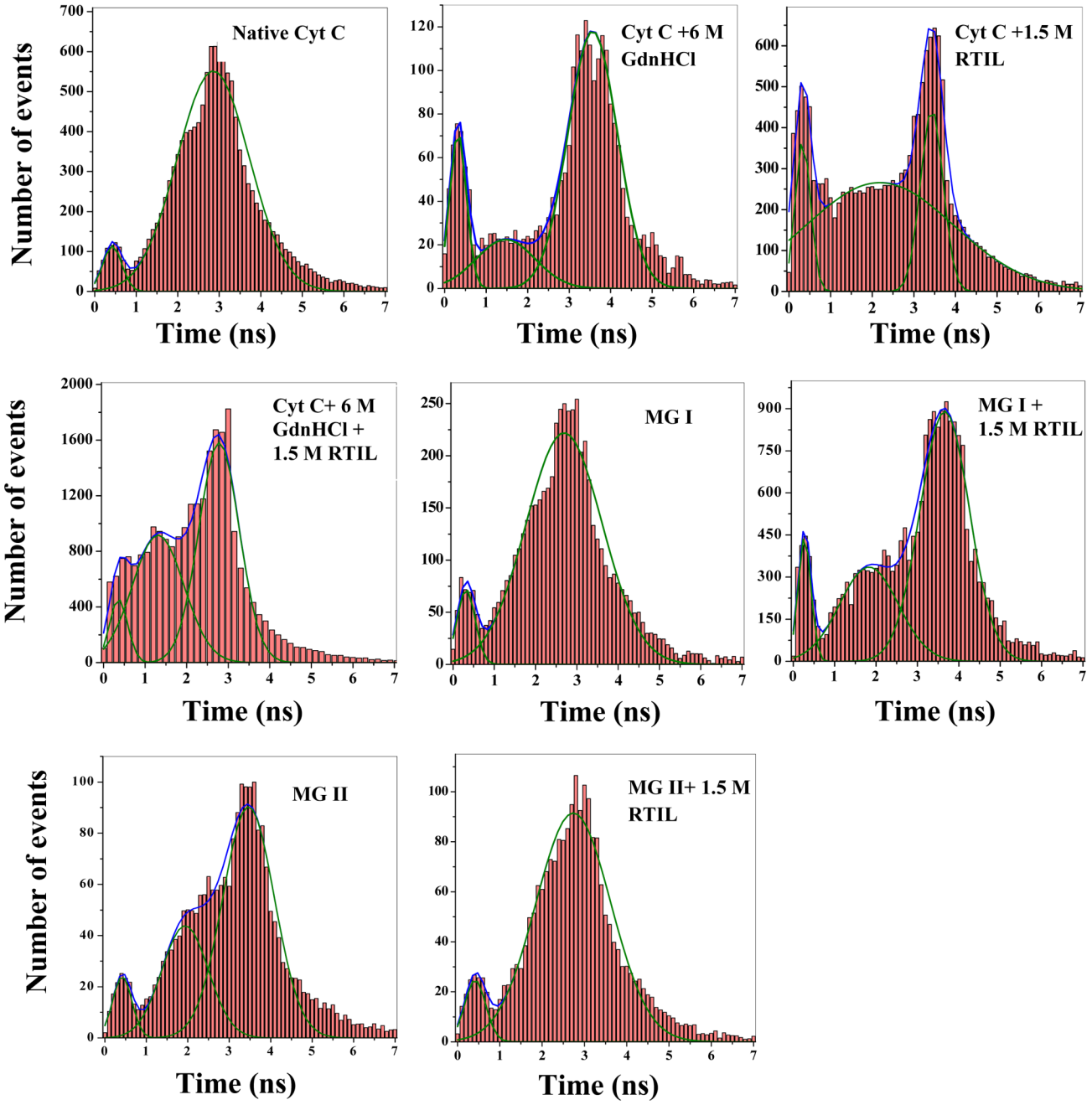

Figure 7. Burst-integrated fluorescence lifetime (BIFL) histograms of Cyt C-Alexa 488 (a) in native state and in the presence of (b) 6 M GdnHCl, (c) 6 M GdnHCl + 1.5 M RTIL, (d) 2 mM SDS (MG-I), (e) MG-I + 1.5 M RTIL, (f) 2 mM SDS + 5 M urea (MG-II), and (g) MG-II + 1.5 M RTIL. Solid blue lines are overall Gaussian fit lines, and the green lines are the Gaussian fit line for the individual lifetime component.

~98 μs (Table 4). In this case the segmental dynamics (3.4 μs) is very close to that (3 μs) in the native state. Thus, the addition of the RTIL to the denatured protein almost completely restores the fast segmental motion to the time constant in native state. The longer component (98 μs), however, remains slower than that (63 μs) in the native state.

3.2.5. Effect of the RTIL on the Conformational Dynamics in the Molten Globule State. For the MG-I state, in the presence of 1.5 M RTIL, the viscosity-corrected time constants of conformational dynamics are 4.5 and 117 μs (Table 5). These are ~1.5−2 fold slower compared to the corresponding relaxation times in the native state. This is consistent with the increase in the size of the protein in MG-I state caused by RTIL.

In contrast to MG-I state, for the molten globule state MG-II, the addition of the RTIL makes the conformational dynamics faster. The viscosity-corrected time constants of MG-II in the presence of 1.5 M RTIL are 3.5 and 85 μs (Table 6) which are very close to those in the native state. This and the RTIL-induced reduction in size suggest the formation of a structure containing native-like compactness.

3.3. Burst Integrated Fluorescence Lifetime (BIFL) Histogram. In the case of Alexa 488 labeled Cyt C, in the native state, the burst integrated lifetime histogram exhibits a distribution with two maxima—at 0.4 ns (5%) and 2.8 ns (95%; Figure 7, Table 7).

When 1.5 M RTIL was added to the native Cyt C we detected three components: 0.3 ns (20%), 2.2 ns (60%), and

dx.doi.org/10.1021/jp307297s | J. Phys. Chem. B 2012, 116, 12189−12198

Table 7. Burst Integrated Fluorescence Lifetime Components

system	τ_1[a] (ns) a_1 %	τ_2[a] (ns) a_2 %	τ_3[a] (ns) a_3 %
native Cyt C	0.4 (5%)		2.8 (95%)
native Cyt C + 6 M GdnHCl	0.3 (14%)	1.4 (16%)	3.6 (70%)
native Cyt C + 1.5 M RTIL	0.3 (20%)	2.2 (60%)	3.6 (20%)
native Cyt C + 6 M GdnHCl + 1.5 M RTIL	0.4 (7%)	1.4 (39%)	2.8 (54%)
native Cyt C + 2 mM SDS (MG-I)	0.3 (7%)		2.8 (93%)
MG-I + 1.5 M RTIL	0.3 (8%)	1.8 (29%)	3.6 (63%)
native Cyt C + 2 mM SDS + 5 M urea (MG-II)	0.4 (7%)	1.8 (28%)	3.6 (65%)
MG-II + 1.5 M RTIL	0.4 (7%)		2.8 (93%)

[a] ±10%.

3.6 ns (20%). All of these components are different from those in the native state.

On addition of 6 M GdnHCl to the protein the magnitude of the shorter component decreases to 0.3 ns. The longer component increases to 3.6 ns. In addition another intermediate component of 1.4 ns (16%) arises in 6 M GdnHCl. Thus, for the protein denatured by 6 M GdnHCl, there are three components: 0.3 ns (14%), 1.4 ns (16%), and 3.6 ns (70%).

Note, two components (0.3 and 3.6 ns) detected in the protein unfolded by GdnHCl are remarkably similar in magnitude (but different in contribution) to those detected in the case of 1.5 M RTIL. This is consistent with the picture that RTIL and GdnHCl both when added separately unfold the protein.

The addition of 1.5 M RTIL to Cyt C denatured by 6 M GdnHCl exhibits three components: 0.4 ns (7%), 1.4 ns (39%), and 2.8 ns (54%). In these, two components (0.4 and 2.8 ns) are identical to those in the native state and suggest refolding of the protein (denatured by GdnHCl) by RTIL.

The MG-I state displays two components: 0.3 ns (7%) and 2.8 ns (93%). When RTIL is added to the MG-I state, the components are 0.3 ns (8%), 1.8 ns (29%), and 3.6 ns (63%).

In the MG-II state, the components are 0.4 ns (7%), 1.8 ns (28%), and 3.6 ns (65%). On addition of 1.5 M RTIL to this (MG-II) molten globule state, the intermediate component vanishes, and only two components are detected: 0.4 ns (7%) and 2.8 ns (93%). These two components are identical to those in the native state and suggest formation of a stable compact native-like structure.

4. DISCUSSION

The fluctuation in fluorescence intensity observed in FCS studies may occur because of two main reasons, diffusion and conformational dynamics. The second source of fluctuation occur may be due to the quenching of the fluorophore emission effectively by the amino groups (Trp, Tyr, Met, or Hist residues) of the protein through PET.[28,29] In all of the cases discussed above, we detected two conformational relaxation components. We now discuss the physical origin of them.

The fastest component, in all cases, is in the range of 3−5.5 μs (after viscosity correction). Many groups assigned the 1−3 μs components to segmental motion.[9,28,29,41−43] It may be noted that Eaton and co-workers suggested that the fastest speed limit of protein folding (i.e., lower limit for the time scale of protein folding) is $\sim N/100$ μs where N denotes the number of residues.[41,42] For horse heart Cyt C, N = 104; according to this formula, the limiting time of protein folding is about 1 μs.[41,42] Thus, our observed time scale (∼3−5.5 μs) is very close to and well within that of the speed limit. For protein folding in ultrafast time scale, Schuler and co-workers reported that a component of 0.7 μs to few microseconds can be present with significant contribution due to Rouse chain dynamics.[43] According to Rouse chain model the time constant of relaxation is given by,

$$\lambda_l = 3D_0\left(\frac{l\pi}{Nb}\right)^2 \qquad l = 1, 3, 5, ...N-1 \tag{10}$$

where N is the number of monomers in the chain, b^2 is mean bond length, and D_0 is the translational diffusion coefficient of the polar residue.[43−45] This time scale depends on the size of the segments taking part in the relaxation. Webb and co-workers also observed a similar 3−8 μs relaxation component for a protein (apomyoglobin) and mentioned it due to contact between probe and proximal amino acid.[9] Following Eaton, Schuler, and Webb and their co-workers we assign the fastest component of 3−5.5 μs corresponds to protein folding or more precisely intrachain contact formation, giving rise to a compact intermediate from which native secondary structures may emerge.

The second component observed in the time scale 63−122 μs is most commonly observed (even by those who used a single component of relaxation[10,11,24,25]) by many groups.[9,24,25,28,29,40−42,46,47] Webb and co-workers observed a similar 30−200 μs component in their study.[9] Werner et al. showed that unfolded Cyt C is in dynamic equilibrium to its intermediate state, and the time scale of conformational fluctuation into and out of the intermediate state is ∼30 μs.[46] Shastry and Roder reported that the protein folding dynamics of Cyt C involves a time scale of ∼50 μs independent of initial conditions and heme ligation state.[47] Hagen and Jones also observed that Met-80 and Met-65 bind to the heme unit at position 18 at a rate of $(40\ \mu s)^{-1}$ and concluded that the Met80-His18 interchain diffusion occurs at ∼35−40 μs time scale in unfolded horse heart Cyt C.[40−42] Majima and co-workers suggested a ∼55 μs time component, while Chattopadhyay and co-workers showed a ∼30 μs component for the collapse of the unfolded protein to a compact structure.[24,25,29] From all of the above-reported results, the 63−122 μs time components may be ascribed to the concerted chain dynamics or motion (interchain diffusion) of the polypeptide side chains of protein.

It may be noted that the magnitude of shorter component of conformational relaxation changes from 3 to 5.5 μs, that is, about 2-fold (Figure 8). The longer time component gradually increases from ∼63 μs in native Cyt C to ∼122 μs in a completely denatured state during protein denaturation (i.e., 2-fold) and subsequently decreases during protein folding. As noted in many earlier reports, the slower components involve diffusion of the protein side chains.[10,11,40−42] Hence, in the unfolded protein, the side chains need to diffuse through a longer path to reach closer to the probe molecule to quench its fluorescence emission (compared to the native state where protein retains a much more compact structure with lower r_H) showing a relatively longer time component.

The heme group in horse heart Cyt C is covalently attached on two of its in-plane corners through Cys14 and Cys17.[26,48] His18 and Met80, axially coordinated to the low spin heme iron, stabilize the native tertiary structure. This Met80 is highly

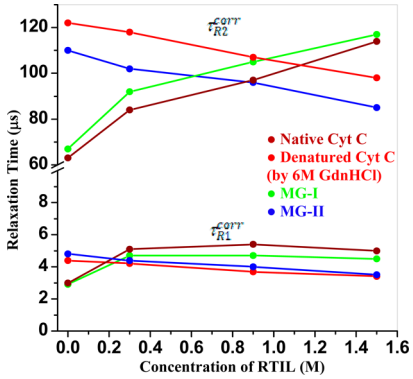

Figure 8. Conformational relaxation time components (viscosity-corrected) are plotted against the concentration of RTIL (M) for (a) native Cyt C (wine), (b) denatured Cyt C (by 6 M GdnHCl) (red), (c) MG-I state (green), and (d) MG-II state (blue).

labile and dissociates in all non-native Cyt C.[26,48] In the presence of a strong denaturing agent such as GdnHCl, the His18 can be replaced by water, while in the presence of RTIL, the Met80 is replaced by the RTIL moiety perturbing the tertiary structure of the protein.[26,48]

In principle, the proteins may deviate from a spherical shape. For an ellipsoid (needle-like shape) Bagchi and co-workers theoretically predicted two translational diffusional coefficients.[49] We have recently followed this in the case of cyclodextrin nanotube aggregates.[50] However the introduction of more than one diffusion coefficient in eq 5 is likely to increase the number of parameters. To get a simplified picture we approximated the protein as a spherical particle. The presence of charge on the protein, Cyt C (positively charged at pH = 7), and electrolytes (RTIL, SDS etc.) may affect translational diffusion ("dielectric friction"), and this may vary with concentration of the electrolyte. This is partially taken into account by taking ratio of the diffusion times of Cyt C and a positively charged dye (R6G) under same diffusing conditions, during size (r_H) measurement (eq 8). We feel the effect of polarization or rotational diffusion of the protein is unimportant for the following reason. The rotational relaxation of a protein ($\eta V/k_BT$) occurs in the time scale of 10−100 ns depending on the size of the protein.[51−55] The rotational relaxation is much faster than the time scale of conformational dynamics (3−120 μs) and diffusion (300−1200 μs).

The most interesting finding of this work is as follows. The RTIL, when added to the native protein or MG-I state (that retains a native-like structural compactness), acts as an denaturant but is the same when added to the fully denatured state (by 6 M GdnHCl) or MG-II state (that almost completely lost the native-like compactness), it acts as an protein stabilizer, decreasing the r_H and, hence, helping the protein to retain a relatively more compact structure. In the native state the more compact protein structure is stabilized by the hydrogen-bonded network. In the presence of a denaturant (GdnHCl or RTIL) the native-like compactness decreases, causing an increase in overall hydrodynamic radius of the protein (from 18.6 Å in native state to 30.3 Å and 25.3 Å in the presence of 6 M GdnHCl and 1.5 M RTIL, respectively). This is because the GdnHCl moiety binds to the surface of protein polypeptide chain and breaks the hydrogen-bonded network that stabilizes the native structure. It also breaks both the axial coordination of the heme unit with His-18 and Met-80, causing almost complete unfolding of the protein. A similar increase in r_H is observed in presence of the RTIL, but it causes partial unfolding of the native structure. In the presence of the RTIL, only the Met-80-heme coordination is ruptured and replaced by the RTIL moiety.[26,48] A similar increase in r_H can also be observed in the presence of other denaturant such as SDS (MG-I state, r_H = 22.4 Å) or both SDS and urea (MG-II state, r_H = 26.4 Å). The RTIL also unfolds the protein when added to the MG-I state (Figure 9). The MG-I state retains most of its

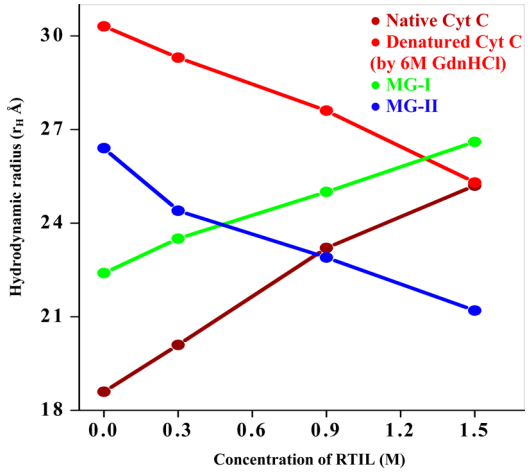

Figure 9. Hydrodynamic radius (r_H) plotted against the concentration of RTIL (M) for (a) native Cyt C (wine), (b) denatured Cyt C (by 6 M GdnHCl) (red), (c) MG-I state (green), and (d) MG-II state (blue).

secondary structure, while the tertiary structure is completely lost. On the other hand, the MG-II state contains 50% of secondary structure with the tertiary structure completely perturbed. This reveals that MG-II has less residual structure or native-like compactness and is more unfolded than MG-I.[30]

When RTIL was added to the fully denatured protein (by 6 M GdnHCl) or MG-II state, we observed a decrease in r_H value (Figure 9). This indicates that the RTIL can stabilize the denatured protein structure and partially restores native-like compactness. This is probably because of strong hydrophobic contact formation between certain residues in the unfolded state on the addition of the RTIL.[42] This leads to a more compact structure, and overall r_H decreases.

The BIFL results also support the above interpretations. According to BIFL data in the native state there are two components of fluorescence lifetime: 0.4 ns (5%) and 2.8 ns (95%). When the protein is denatured by GdnHCl or by the RTIL, these components change appreciably, implying a marked change in the local or microenvironment around the probe (Alexa). However, when the protein retains a relatively compact native-like structure (e.g., by addition of the RTIL to GdnHCl denatured protein or to MG-II), the 0.4 and 2.8 ns components are restored.

5. CONCLUSION

The FCS study shows a substantial difference in the size and conformational dynamics of native, denatured, and molten globule states (I and II) of Cyt C. The MG-I state displays conformational dynamics similar to those in the native state. But, the relaxation dynamics of MG-II state is ∼2 fold slower compared to the native state. When GdnHCl (or RTIL) are added separately to the protein, the latter is denatured which is

dx.doi.org/10.1021/jp307297s | J. Phys. Chem. B 2012, 116, 12189−12198

manifested in the increase in size and magnitude of time constant of conformational relaxation and also the change in fluorescence lifetime components (as detected by BIFL). However, when the protein is refolded by the addition of RTIL to the protein denatured by GdnHCl or to MG-II state, the native-like size, relaxation components, and fluorescence lifetimes are recovered.

AUTHOR INFORMATION

Corresponding Author

*E-mail: pckb@iacs.res.in. Phone: (91)-33-2473-3542. Fax: (91)-33-2473-2805.

Notes

The authors declare no competing financial interest.

ACKNOWLEDGMENTS

Thanks are due to the Department of Science and Technology, India (Centre for Ultrafast Spectroscopy and Microscopy Project and J. C. Bose Fellowship) and the Council of Scientific and Industrial Research (CSIR) for generous research support. S.S.M., R.C., and S.C. thank CSIR for awarding fellowships.

REFERENCES

(1) Kim, H. D.; Nienhaus, G. U.; Ha, T.; Orr, J. W.; Williamson, J. R.; Chu, S. *Proc. Natl. Acad. Sci. U.S.A.* **2002**, *99*, 4284−4289.

(2) Kim, J.; Doose, S.; Neuweiler, H.; Sauer, M. *Nucleic Acids Res.* **2006**, *34*, 2516−2527.

(3) Li, H. T.; Ren, X. J.; Ying, L. M.; Balasubramanian, S.; Klenerman, D. *Proc. Natl. Acad. Sci. U.S.A.* **2004**, *101*, 14425−14430.

(4) Wallace, M. I.; Ying, L. M.; Balasubramanian, S.; Klenerman, D. *J. Phys. Chem. B* **2000**, *104*, 11551−11555.

(5) Edman, L.; Mets, U.; Rigler, R. *Proc. Natl. Acad. Sci. U.S.A.* **1996**, *93*, 6710−6715.

(6) Jung, J.; Orden, A. V. *J. Am. Chem. Soc.* **2006**, *128*, 1240−1249.

(7) Jung, J.; Orden, A. V. *J. Phys. Chem. B* **2005**, *109*, 3648−3657.

(8) Neuweiler, H.; Doose, S.; Sauer, M. *Proc. Natl. Acad. Sci. U.S.A.* **2005**, *102*, 16650−16655.

(9) Chen, H.; Rhoades, E.; Butler, J. S.; Loh, S. N.; Webb, W. W. *Proc. Natl. Acad. Sci. U.S.A.* **2007**, *104*, 10459−10464.

(10) Chattopadhyay, K.; Elson, E. L.; Frieden, C. *Proc. Natl. Acad. Sci. U.S.A.* **2005**, *102*, 2385−2389.

(11) Chattopadhyay, K.; Saffarian, S.; Elson, E. L.; Frieden, C. *Proc. Natl. Acad. Sci. U.S.A.* **2002**, *99*, 14171−14176.

(12) Rischel, C.; Jorgensen, L. E.; Foldes-Papp, Z. *J. Phys.: Condens. Matter* **2003**, *15*, S1725−S1735.

(13) Margittai, M.; Widengren, J.; Schweinberger, E.; Schroder, G. F.; Felekyan, S.; Haustein, E.; Konig, M.; Fasshauer, D.; Grubmuller, H.; Jahn, R.; Seidel, C. A. M. *Proc. Natl. Acad. Sci. U.S.A.* **2003**, *100*, 15516−15521.

(14) Werner, J. H.; Joggerst, R.; Dyer, R. B.; Goodwin, P. M. *Proc. Natl. Acad. Sci. U.S.A.* **2006**, *103*, 11130−11135.

(15) Sasmal, D. K.; Mondal, T.; Sen Mojumdar, S.; Choudhury, A.; Banerjee, R.; Bhattacharyya, K. *J. Phys. Chem. B* **2011**, *115*, 13075−13083.

(16) Liu, R.; Hu, D.; Tan, X.; Lu, H. P. *J. Am. Chem. Soc.* **2006**, *128*, 10034−10042.

(17) Nettels, D.; Hoffmann, A.; Schuler, B. *J. Phys. Chem. B* **2008**, *112*, 6137−6146.

(18) Ziv, G.; Haran, G. *J. Am. Chem. Soc.* **2009**, *131*, 2942−2947.

(19) Chi, Q. J.; Farver, O.; Ulstrup, J. *Proc. Natl. Acad. Sci. U.S.A.* **2005**, *102*, 16203−16208.

(20) Furukawa, Y.; Ban, T.; Hamada, D.; Ishimori, K.; Goto, Y.; Morishima, I. *J. Am. Chem. Soc.* **2005**, *127*, 2098−2103.

(21) Yang, H.; Luo, G.; Karnchanaphanurach, P.; Louie, T. M.; Rech, I.; Cova, S.; Xun, L.; Xie, X. S. *Science* **2003**, *302*, 262−266.

(22) Tan, X.; Nalbant, P.; Toutchkine, A.; Hu, D.; Vorpagel, E. R.; Hahn, K. M.; Lu, H. P. *J. Phys. Chem. B* **2004**, *108*, 737−744.

(23) Xie, X. S. *J. Chem. Phys.* **2002**, *117*, 11024−11032.

(24) Haldar, S.; Mitra, S.; Chattopadhyay, K. *J. Biol. Chem.* **2010**, *285*, 25314−25323.

(25) Haldar, S.; Chattopadhyay, K. *J. Biol. Chem.* **2012**, *287*, 11546−11555.

(26) Oellerich, S.; Wackerbarth, H.; Hildebrandt, P. *J. Phys. Chem. B* **2002**, *106*, 6566−6580.

(27) Hildebrandt, P.; Stockburger, M. *Biochemistry* **1989**, *28*, 6722−6728.

(28) Chen, H.; Ahsan, S. S.; Santiago-Berrios, M. B.; Abruna, H. D.; Webb, W. W. *J. Am. Chem. Soc.* **2010**, *132*, 7244−7245.

(29) Choi, J.; Kim, S.; Tachikawa, T.; Fujitsuka, M.; Majima, T. *Phys. Chem. Chem. Phys.* **2011**, *13*, 5651−5658.

(30) Chattopadhyay, K.; Mazumdar, S. *Biochemistry* **2003**, *42*, 14606−14613.

(31) Soares, C. M.; Baptista, A. M. *FEBS Lett.* **2012**, *586*, 510−518.

(32) Singh, S. R.; Prakash, S.; Muneeswaran, G.; Rajesh, S.; Muthukumar, K.; Vasu, V.; Karunakaran, C. *Mol. Simul.* **2012**, *38*, 459−467.

(33) Kam, N. W. S.; Dai, H. *J. Am. Chem. Soc.* **2005**, *127*, 6021−6026.

(34) Petrasek, Z.; Schwille, P. *Biophys. J.* **2008**, *94*, 1437−1448.

(35) Chattopadhyay, K.; Saffarian, S.; Elson, E. L.; Frieden, C. *Biophys. J.* **2005**, *88*, 1413−1422.

(36) Sherman, E.; Itkin, A.; Kuttner, Y. Y.; Rhoades, E.; Amir, D.; Haas, E.; Haran, G. *Biophys. J.* **2008**, *94*, 4819−4827.

(37) Wilkins, D. K.; Grimshaw, S. B.; Receveur, V.; Dobson, C. M.; Jones, J. A.; Smith, L. J. *Biochemistry* **1999**, *38*, 16424−16431.

(38) Baker, S. N.; Zhao, H.; Pandey, S.; Heller, W. T.; Bright, F. V.; Baker, G. A. *Phys. Chem. Chem. Phys.* **2011**, *13*, 3642−3644.

(39) Constantinescu, D.; Weingärtner, H.; Herrmann, C. *Angew. Chem., Int. Ed.* **2007**, *46*, 8887−8889.

(40) Jones, C. M.; Henry, E. R.; Hu, Y.; Chan, C. K.; Luck, S. D.; Bhuyan, A.; Roder, H.; Hofrichter, J.; Eaton, W. A. *Proc. Natl. Acad. Sci. U.S.A.* **1993**, *90*, 11860−11864.

(41) Kubelca, J.; Hofrichter, J.; Eaton, W. A. *Curr. Opin. Struct. Biol.* **2004**, *14*, 76−88.

(42) Hagen, S. J.; Hofrichter, J.; Szabo, A.; Eaton, W A. *Proc. Natl. Acad. Sci. U.S.A.* **1996**, *93*, 11615−11617.

(43) Soranno, A.; Buchli, B.; Nettels, D.; Cheng, R. R.; Spath, S. M.; Pfeil, S. H.; Hoffman, A.; Lipman, E. A.; Makarov, D. E.; Schuler, B. *Proc. Natl. Acad. Sci. U.S.A.* **2012**, DOI: 10.1073/pnas.1117368109.

(44) Das, D. K.; Mondal, T.; Mandal, U.; Bhattacharyya, K. *ChemPhysChem* **2010**, *12*, 814−822.

(45) Doi, S.; Edwards, F. *The Theory of Polymer Dynamics*; Oxford University Press: Oxford, U.K., 1986.

(46) Werner, J. H.; Joggerst, R.; Dyer, R. B.; Goodwin, P. M. *Proc. Natl. Acad. Sci. U.S.A.* **2006**, *103*, 11130−11135.

(47) Shastry, M. C. R.; Roder, H. *Nat. Struct. Biol.* **1998**, *5*, 385−392.

(48) Bihari, M.; Russell, T. P.; D. Hoagland, A. *Biomacromolecules* **2010**, *11*, 2944−2948.

(49) Vasanthi, R.; Ravichandran, S.; Bagchi, B. *J. Chem. Phys.* **2001**, *114*, 7989−7992.

(50) Mandal, A. K.; Das, D. K.; Das, A. K.; Sen Mojumdar, S.; Bhattacharyya, K. *J. Phys. Chem. B* **2011**, *115*, 10456−10461.

(51) Nandi, N.; Bagchi, B. *J. Phys. Chem. A* **1998**, *102*, 8217−8221.

(52) Jordanides, X. J.; Lang, M. J.; Song, X.; Fleming, G. R. *J. Phys. Chem. B* **1999**, *103*, 7995−8005.

(53) Nandi, N.; Bhattacharyya, K.; Bagchi, B. *Chem. Rev.* **2000**, *100*, 2013−2046.

(54) Matyushov, D. V.; Morozov, A. Y. *Phys. Rev. E* **2011**, *84*, 011908-1−10.

(55) Leontyev, I. V.; Stuchebrukhov, A. A. *J. Chem. Phys.* **2009**, *130*, 085103-1−15.